Article

Journal of Nanoscience and Nanotechnology
Vol. 19, 6668–6674, 2019
www.aspbs.com/jnn

Silicon-on-Insulator Double-Gate Ion-Sensitive Field-Effect Transistors Using Flexible Paper Substrate-Based Extended Gate for Cost-Effective Sensor Applications

Jin-Hyeok Jeon and Won-Ju Cho*

Department of Electronic Materials Engineering, Kwangwoon University, Seoul 01897, Republic of Korea

We developed ion-sensitive field effect transistors (ISFETs) with disposable paper extended gates (EGs). The sensing and the measuring part of conventional ISFETs are not separated and integrated on the same device. Therefore, if the sensing part is contaminated by reaction in a chemical solution, there is a problem that an expensive measuring part manufactured through a complicated process becomes also unusable. To overcome this problem and provide a cost-effective sensor platform, we constructed a high-sensitivity ISFET sensor with a measuring transistor part and a separate EG sensing part. In particular, in this experiment, a double-gate transistor capable of amplifying the sensitivity using the capacitive coupling effect between a top-gate and a bottom-gate, which differs from a general single gate transistor on an SOI substrate, was fabricated. As a result, the pH sensitivity of 1199.92 ± 32.4 mV/pH could be achieved using paper EG and dual-gate mode sensing operation, which greatly exceeds the theoretical Nernst limit (59.15 mV/pH at 25 °C) in single gate mode sensing operation. We also measured non-ideal effects such as the hysteresis and drift behavior of paper EGs, and demonstrated that they have excellent stability and reliability for long-term measurements. In addition, hysteresis and sensitivity were measured after 3, 7, 14 and 30 days to verify the aging effect of the continuous use of paper EGs. As a result, paper EGs showed stable operating characteristics for 30 days. Therefore, we expect that double-gate ISFETs with flexible paper EGs will have a significant impact on label-free, low-environmental impact, cost-effective, disposable, and flexible FET-based biosensor applications.

Keywords: Paper Extended Gate, Double-Gate Ion-Sensitive Field Effect Transistors, Capacitive Coupling, pH Sensor, Cost-Effective, Disposable, Dual Gate Mode Sensing.

1. INTRODUCTION

Recently, biosensors have been actively studied with promising technologies in various fields, such as environmental, medical, biomimetic, analytical chemistry technologies because of their capability of quick and accurate analysis [1–4]. The biosensor platform converts biological reactions into detectable electrical signals. Biosensors consist of biomaterials and transducers. Examples of biomaterials include not only pH, but also cells, antigen-antibodies, DNA, and enzymes. Transducers that convert biological elements into detectable signals use a variety of physical and chemical methods such as fluorescence, field-effect transistors (FETs), surface plasma resonance (SPR), electrochemistry, and thermal sensors. Among the various types of biosensors, FET-based biosensors have attracted much attention because they have advantages in terms of small size, fast and accurate detection, robustness, portability, label-free processing, and compatibility with CMOS processes [5–10]. A typical FET-based biosensor is the ion-sensitive field effect transistor (ISFET) proposed by Bergveld in the 1970s. The structure of ISFETs is based on conventional metal–oxide–semiconductor FETs (MOSFETs). Instead of the gate electrode of the conventional MOSFET, ISFETs have different structures for the electrolyte and reference electrode [11]. Namely, ISFETs can be used as pH sensors,

*Author to whom correspondence should be addressed.

 1533-4880/2019/19/6668/007 doi:10.1166/jnn.2019.17096

since the ion concentration in the solution is detected by the surface potential change due to the ionic reaction on the surface of the gate insulator [12–13]. However, conventional ISFETs are difficult to commercialize due to the difficulty they face in detecting low-amplitude biological signals, such as those from cells, antigen-antibodies, DNA, and enzymes, because the sensitivity of ISFETs is limited by the theoretical Nernst sensitivity limit (59.15 mV/pH at 25 °C) [14]. The ISFET sensors consist of a sensing part and a measuring part in the same device. In particular, the sensing part is easily damaged because it is directly exposed to the chemical solution. As a result, there is a problem in that the entire ISFET, including the measurement unit, becomes unusable, which is disadvantageous in terms of cost efficiency.

In order to solve these fundamental problems, in this study, we have introduced two concepts: (1) a double-gate FET and (2) an extended gate (EG) into a measuring part and a sensing part, respectively. A double-gate FET is useful to overcome the Nernst sensitivity limit by using capacitive coupling between the top- and bottom-gates of the fully depleted channel without using additional amplifiers [15–20]. On the other hand, the EG was separated from the measuring transistor part [21–24] and fabricated using a low-cost paper substrate. Paper has various advantages, such as flexibility, cost-effectiveness, eco-friendliness, disposability, and a simple fabrication process [25–29]. Thus, replacing a damaged disposable EG detector has the advantage of being able to continue to use the double-gate FET transducer cost-effectively. We measured the pH sensitivity after connecting the double-gate FET transducer to the paper EG detector. In addition, to evaluate the stability and reliability of the paper EG in the electrolyte, the hysteresis and drift effects were evaluated. Finally, in order to verify the aging effect of continuous use of the paper EG, hysteresis and sensitivity after 3, 7, 14, and 30 days were measured.

2. EXPERIMENTAL DETAILS

To fabricate a double-gate FET as a transducer part, a *p*-type (100) silicon-on-insulator (SOI) wafer with a top-silicon layer of 30 nm thickness and a buried oxide (BOX) layer of 750 nm thickness was used. The resistivity and the boron doping concentration of the top-silicon layer were 10 $\Omega \cdot cm$ and 1×10^{15} cm^{-3}, respectively, which satisfies the conditions of fully depleted channel formation for capacitive coupling in the double-gate FET. After the active region was formed using photolithography and a reactive ion-etching (RIE) process, a 100-nm-thick phosphorus-doped poly-Si layer was deposited on the source/drain (S/D) regions using low pressure chemical vapor deposition (LPCVD) at 650 °C. A 20-nm-thick SiO_2 layer was then deposited on the top-silicon layer using RF magnetron sputtering, which served as the top-gate insulator of the double-gate TFT, while the 750-nm-thick BOX layer served as the bottom-gate insulator. To improve the conductivity of the phosphorus-doped poly-Si S/D electrode, rapid thermal annealing (RTA) was performed at 950 °C for 30 s in N_2/O_2 ambient gas. Finally, an Al gate electrode was formed with a thickness of 150 nm using an electron beam evaporator, followed by gas annealing at 450 °C for 30 m in a 5% H_2/N_2 atmosphere. A schematic of a dual-gate FET transducer implemented on an SOI substrate is shown in Figure 1(a). Further, we used cellulose paper (manufacturer: OKclean RN), which has a compact structure as a substrate for an EG detector, with flexibility, cost-effectiveness, eco-friendliness, disposability, and simple fabrication. A microscope image of the cellulose paper surface is shown in Figure 1(b). After depositing a 100-nm-thick Al_2O_3 insulating layer on a paper substrate, waterproof layer was coated by polyethylene wax to protect soaking the paper substrate form pH solution, and a 300-nm-thick ITO conductive layer was deposited to transfer the potential change of the sensing membrane surface to the double-gate FET transducer. As the sensing film of

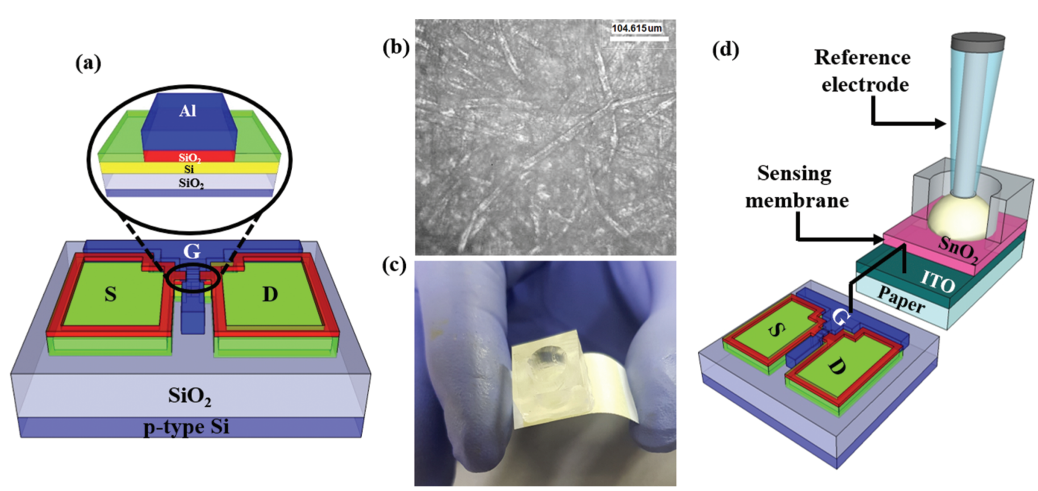

Figure 1. (a) Schematic of the SOI MOSFETs. (b) Microscope image of cellulose paper surface. (c) Photograph of flexible paper substrate-based EG. (d) Schematic diagram of a double-gate ISFET with a paper EG detector directly connected to an SOI MOSFET transducer.

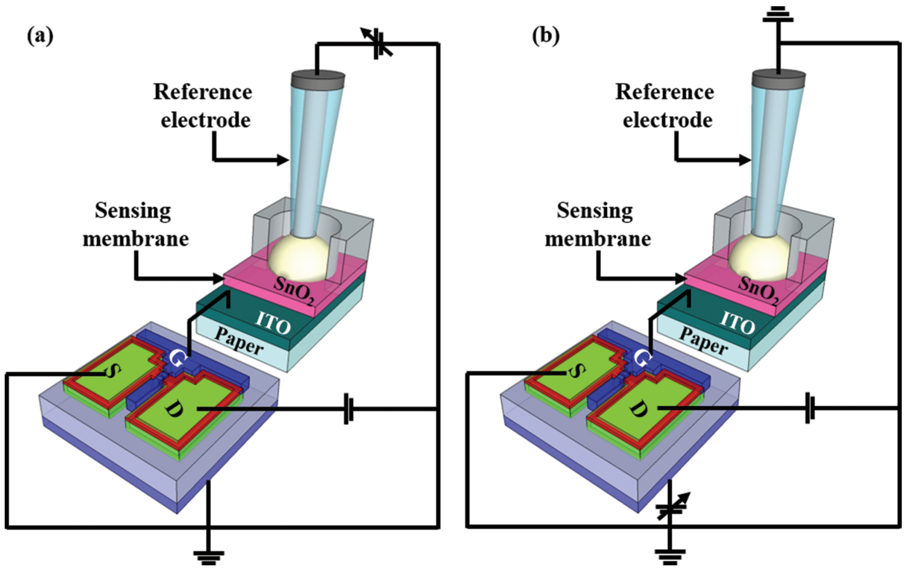

Figure 2. Schematics of measurement for (a) SG mode sensing and (b) DG mode sensing.

the EG detector, a 50-nm-thick SnO_2 thin film with outstanding pH sensitivity and reliability was deposited by RF sputtering [30]. Finally, a polydimethylsiloxane (PDMS) reservoir with an internal diameter of 0.6 cm for injection of the pH buffer solution was attached to the sensing buffer using a silicone glue. A photograph of the flexible paper substrate-based EG is shown in Figure 1(c). The ITO electrode of the EG detector was connected directly to the top-gate electrode of the SOI MOSFETs. A schematic of a double-gate ISFET with a paper EG detector directly connected to an SOI MOSFET transducer is shown in Figure 1(d).

The sensing of all electrical properties and pH of the fabricated devices was performed in the dark box to the avoid effects of light and the external environment, using an Agilent 4156B precision semiconductor parameter analyzer. The Ag/AgCl reference electrode (Horiba 2080A-06T with a ceramic-plug junction and an internal solution saturated with KCl and AgCl) was used to measure the pH sensitivity of the sensor for various pH buffer solutions. The fabricated ISFET evaluated the pH sensitivity by two methods: single gate (SG) mode and dual gate (DG) mode, as shown in Figure 2. SG mode sensing was conducted by sweeping the reference electrode bias voltage while the BG was grounded. In contrast, DG mode sensing was performed by sweeping the BG bias voltage while grounding the upper reference electrode.

3. RESULTS AND DISCUSSION

To amplify the pH sensing capability by using the capacitive coupling effect between the double gates, the SOI MOSFETs must be independently operated by the top-gate or the bottom-gate. Figures 3(a) and (b) show the transfer characteristics ($I_D - V_G$) of the SOI based double-gate MOSFETs operated with the top-gate and bottom-gate, respectively.

It can be seen that the SOI MOSFETs fabricated for the transducers of the ISFET sensor exhibit good transfer characteristics for both top-gate and bottom-gate operation. Under the operating conditions of the top-gate only, it exhibits a threshold voltage of −0.28 V, a subthreshold swing of 74.80 mV/dec, and an on/off current ratio of

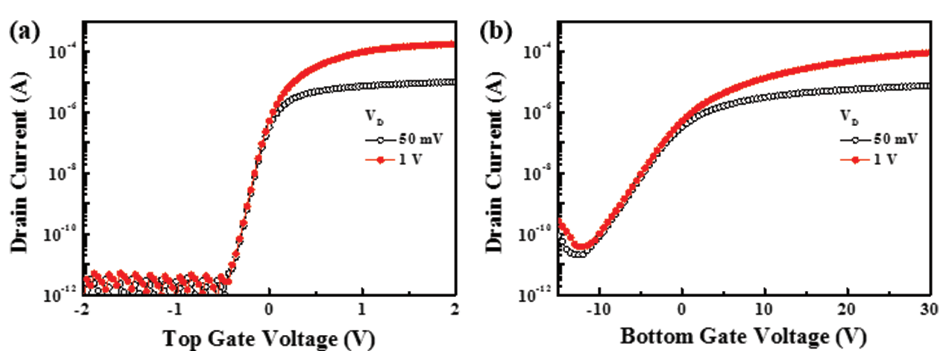

Figure 3. Transfer characteristic curves of SOI based double-gate MOSFETs in (a) top-gate and (b) bottom-gate operations.

Table I. Electrical parameters of the fabricated SOI MOSFETs under top-gate or bottom-gate operation.

Operating mode	Threshold voltage (V)	Subthreshold swing (mV/dec)	On/off current ratio
Top-gate	−0.28	74.8	6.51×10^7
Bottom-gate	−9.23	2541.71	2.41×10^6

6.51×10^7. On the other hand, under the operating conditions of the bottom-gate only, it exhibits a threshold voltage of −9.23 V, a subthreshold swing of 2541.7 mV/dec, and an on/off current ratio of 2.41×10^6. Table I summarizes the electrical parameters of the fabricated SOI based double-gate MOSFETs under top-gate or bottom-gate operation. Figure 4 shows the sensing characteristics of a double-gate ISFET using a paper-based EG detector. Figures 4(a) and (b) show the transfer curves of the SG and DG modes, respectively, for various pH buffer solutions. The transfer characteristic curve shifts to the right direction (positive gate voltage) as the pH of the buffer solution increases. In addition, the amount of shift in the DG mode is much larger than that in the SG mode for the same pH level change. In this study, we defined 1 nA as the reference current (I_R) and the voltage corresponding to I_R as the reference voltage (V_R).

Figure 5 shows the pH sensitivity calculated from the slope ($\Delta V_R/\Delta$pH) of the V_R with respect to the measured pH buffer solutions. The pH sensitivity was 55.97 ± 1.26 mV/pH in the SG mode and is close to the Nernst limit of approximately 59.15 mV/pH. On the other hand, in the DG mode, the sensitivity was 1199.92 ± 32.4 mV/pH, which is about 21 times higher than that of the SG mode. This sensitivity amplification is maximized when the capacitance of the top-gate oxide is much larger than that of the bottom-gate oxide. The sensitivity and the capacitive coupling relationships in double-gate ISFETs are described by following equation [16]:

$$\Delta V_{th}^{B} = \frac{C_{Si} C_{tox}}{C_{box}(C_{Si} + C_{tox})} \quad \Delta V_{th}^{T} = \frac{3t_{box}}{3t_{tox} + t_{Si}} \Delta V_{th}^{T} \qquad (1)$$

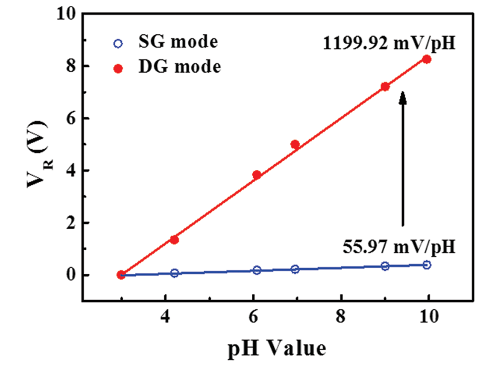

Figure 5. Change in V_R as a function of pH value. The reference voltage (V_R) of the sensor for each pH buffer solution was defined as the corresponding gate voltage to the drain current (reference current I_R) of 1 nA.

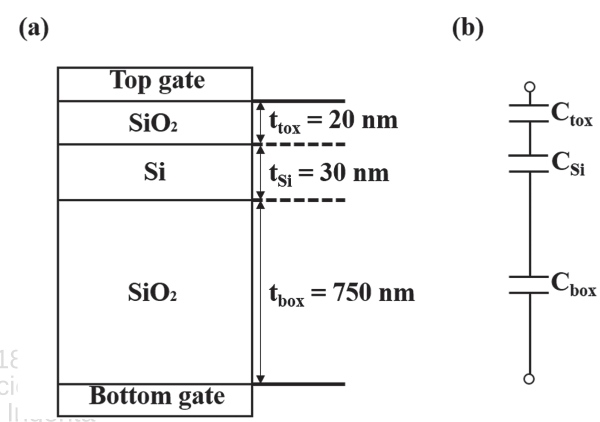

Figure 6. (a) The MOSCAP structure of SOI MOSFETs. (b) The equivalent circuit of SOI MOSFETs in the DG mode.

where C_{Si}, C_{tox}, and C_{box} are the capacitance per unit area of the channel, top-gate oxide, and bottom-gate oxide, respectively; and t_{Si}, t_{tox}, and t_{box} are the thickness of the channel, top-gate oxide, and bottom-gate oxide which are shown in Figures 6(a) and (b), respectively. Figure 6(a) shows the MOSCAP structure of SOI MOSFETs and Figure 6(b) shows the equivalent circuit of SOI MOSFETs in the DG mode. In other words, according to

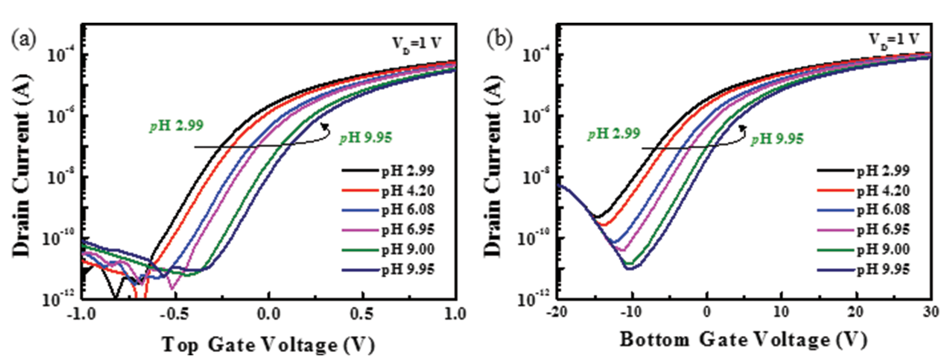

Figure 4. Sensing characteristics of a double-gate ISFET using a paper-based EG detector for various pH buffer solutions: The transfer curves of (a) SG mode and (b) DG mode.

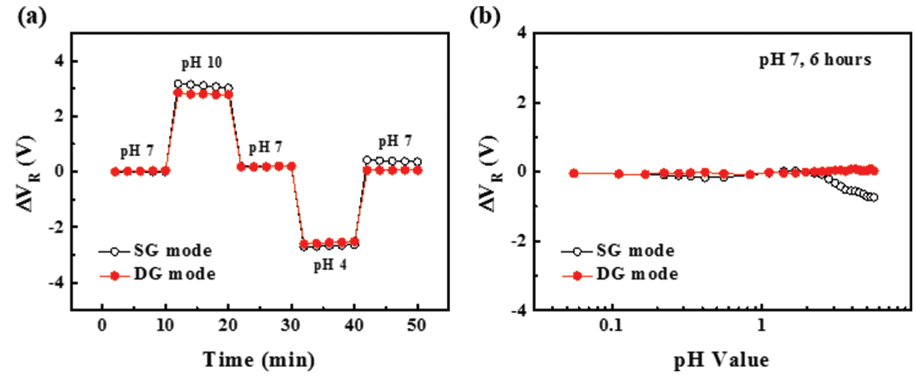

Figure 7. Non-ideal behavior of double-gate ISFET using paper EG detector: (a) Hysteresis and (b) drift characteristics.

Table II. Comparison of the pH sensing performance parameters of DG ISFETs using paper EGs.

Sensing mode	Sensitivity [mV/pH]	Linearity [%]	Hysteresis voltage (V_H) [mV]	Drift rate [mV/pH]
SG mode	55.97 ± 1.26	99.94	20.18	7.18
DG mode	1199.92 ± 32.4	99.78	70.95	22.99

$C_{Si}C_{tox}/C_{box}(C_{Si}+C_{tox})$, the sensitivity is amplified in the DG mode, which is converted into the gate oxide and channel thickness, and is then $3t_{box}/3t_{tox}+t_{Si}$. Since the t_{box}, t_{tox} and t_{Si} of the fabricated SOI MOSFETs are 750, 20, and 30 nm, respectively, the theoretical sensitivity can be amplified to about 25 times. This is similar to the experimental sensitivity amplification.

We evaluated the reliability and stability of paper EG detectors by measuring non-ideal behavior, such as hysteresis and drift effects. Typically, hysteresis occurs due to the changing amount of micro-charging charge caused by the slow reaction of the sensing membrane surface with ions in the electrolyte, resulting in a change in the V_R [31]. We measured the hysteresis in a pH loop of $7 \rightarrow 10 \rightarrow 7 \rightarrow 4 \rightarrow 7$ by directly immersing the paper EG detector into buffer solutions. The hysteresis width was then defined as the difference in V_R between the starting pH 7 solution and the final pH 7 solution in the pH loop. In addition, the drift effect indicates the change in V_R due to the amount of charge that changes as ions penetrate into the sensing membrane when the surface of the sensing membrane is exposed to the electrolyte for a long time [32].

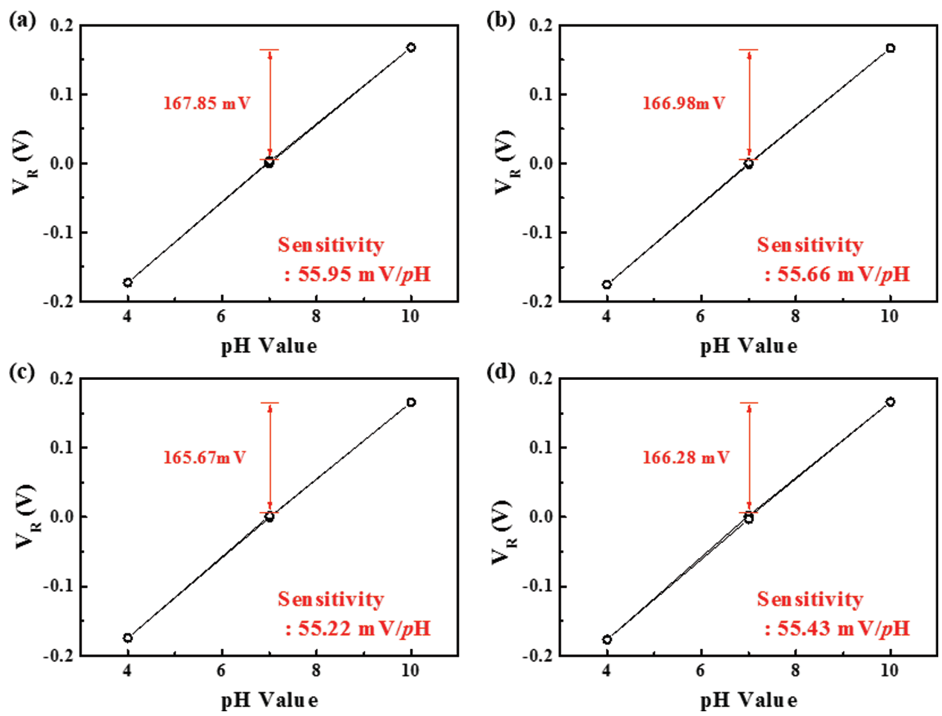

Figure 8. Aging effects on the residual plot of the hysteresis curve, hysteresis width, and sensitivity in the hysteresis pH loop (a) after 3 days, (b) after 7 days, (c) after 14 days, and (d) after 30 days.

We investigated the drift characteristics by observing the shift of V_R in a buffer solution of pH 7 over a period of 6 h to evaluate the long-term chemical stability of the fabricated pH sensors. Figures 7(a) and (b) show the hysteresis and drift effect in the SG and DG mode, respectively. It is found that the hysteresis voltage (V_H) and the drift rate in the DG mode are increased by about 3 times as compared with those of the SG mode. This means that the increase in hysteresis and drift is relatively small, considering that the sensitivity is increased about 21 times in the DG mode compared to the SG mode. That is, the DG mode is improved in terms of stability and reliability of measurement compared to the SG mode. This is because the thickness of the bottom-gate oxide is thicker than that of the top-gate oxide of the SOI MOSFET, and the stress of the vertical electric field applied to the Si channel is reduced [33]. The pH sensing parameters of the ISFET in the SG mode and DG mode are summarized in Table II.

Paper-based electronic devices have advantages such as flexibility, cost-effectiveness, eco-friendliness, disposability, and a simple fabrication process. However, since paper is susceptible to chemical and physical damage, paper-based EG detectors have concerns regarding durability and sensitivity. We evaluated hysteresis and sensitivity after 3, 7, 14, and 30 days to confirm the aging effect of the continuous use of paper-based EG detectors. Figure 8 shows the hysteresis curve, hysteresis width, and sensitivity of the hysteresis pH loop after (a) 3 days, (b), 7 days, (c), 14 days, (d), and 30 days. It is found that the paper-based EG has a stable hysteresis width and sensitivity for 30 days, indicating that the pH can be detected stably. This means that the pH-sensing capability of paper-based EG detectors is maintained without deterioration.

4. CONCLUSION

In this study, we developed an ISFET with a disposable paper EG detector. To overcome the problems of conventional ISFET sensors and to provide a cost-effective sensor platform, we constructed a highly sensitive ISFET sensor consisting of a dual-gate SOI MOSFET converter part and a separate EG detector part. The dual-gate SOI-based transducer was able to achieve a pH sensitivity of 1199.92 ± 32.4 mV/pH, far exceeding the theoretical Nernst limit of conventional single-gate ISFETs (59.15 mV/pH at 25 °C). This is because the sensitivity is greatly amplified by the capacitive coupling effect between the top gate and the bottom gate of the double gate. We have also measured non-ideal effects, such as hysteresis and drift behavior of paper EG detectors, and have demonstrated excellent stability and reliability for long-term measurements. In addition, the aging effect of the continuous use of paper EGs was evaluated, which showed stable operation characteristics for 30 days. Therefore, double-gate ISFETs using flexible paper EGs are expected to be useful in label-free, low-environmental impact, cost-effective disposable, and flexible FET-based biosensor applications.

Acknowledgments: This study was supported by the Basic Science Research Program through the National Research Foundation of Korea (NRF), funded by the Ministry of Education, Science, and Technology (No. 2016R1A2B4008754), and conducted with the support of the business Start-up Technology Development Project funded by the Small and Medium Business Administration (SMBA, Korea) in 2016 (Grant No.: S2409184) and this research was funded and conducted under the Competency Development Program for Industry Specialists of the Korean Ministry of Trade, Industry and Energy (MOTIE), operated by Korea Institute for Advancement of Technology (KIAT) (No. P0002397, HRD program for Industrial Convergence of Wearable Smart Devices).

References and Notes

1. Wang, J., Cai, X., Rivas, G., Shiraishi, H., Farias, P.A. and Dontha, N., **1996**. DNA electrochemical biosensor for the detection of short DNA sequences related to the human immunodeficiency virus. *Analytical Chemistry, 68*(15), pp.2629–2634.
2. Wang, B., Li, B., Deng, Q. and Dong, S., **1998**. Amperometric glucose biosensor based on sol–gel organic–inorganic hybrid material. *Analytical Chemistry, 70*(15), pp.3170–3174.
3. Meric, B., Kerman, K., Ozkan, D., Kara, P., Erensoy, S., Akarca, U.S., Mascini, M. and Ozsoz, M., **2002**. Electrochemical DNA biosensor for the detection of TT and Hepatitis B virus from PCR amplified real samples by using methylene blue. *Talanta, 56*(5), pp.837–846.
4. Torbicz, W. and Pijanowska, D.G., **1997**. pH-ISFET based urea biosensor. Sensors & Actuators: B. *Chemical, 1*(44), pp.370–376.
5. Bergveld, P., **1986**. The development and application of FET-based biosensors. *Biosensors, 2*(1), pp.15–33.
6. Simonian, A.L., Flounders, A.W. and Wild, J.R., **2004**. FET-based biosensors for the direct detection of organophosphate neurotoxins. *Electroanalysis: An International Journal Devoted to Fundamental and Practical Aspects of Electroanalysis, 16*(22), pp.1896–1906.
7. Kim, D.S., Park, J.E., Shin, J.K., Kim, P.K., Lim, G. and Shoji, S., **2006**. An extended gate FET-based biosensor integrated with a Si microfluidic channel for detection of protein complexes. *Sensors and Actuators B: Chemical, 117*(2), pp.488–494.
8. Kim, D.S., Jeong, Y.T., Park, H.J., Shin, J.K., Choi, P., Lee, J.H. and Lim, G., **2004**. An FET-type charge sensor for highly sensitive detection of DNA sequence. *Biosensors and Bioelectronics, 20*(1), pp.69–74.
9. Anh, T.M., Dzyadevych, S.V., Soldatkin, A.P., Chien, N.D., Jaffrezic-Renault, N. and Chovelon, J.M., **2002**. Development of tyrosinase biosensor based on pH-sensitive field-effect transistors for phenols determination in water solutions. *Talanta, 56*(4), pp.627–634.
10. Liu, S. and Guo, X., **2012**. Carbon nanomaterials field-effect-transistor-based biosensors. *NPG Asia Materials, 4*(8), p.e23.
11. Bergveld, P., **1972**. Development, operation, and application of the ion-sensitive field-effect transistor as a tool for electrophysiology. *IEEE Transactions on Biomedical Engineering*, (5), pp.342–351.
12. Chou, J.C. and Liao, L.P., **2005**. Study on pH at the point of zero charge of TiO_2 pH ion-sensitive field effect transistor made by the sputtering method. *Thin Solid Films, 476*(1), pp.157–161.
13. Chin, Y.L., Chou, J.C., Sun, T.P., Liao, H.K., Chung, W.Y. and Hsiung, S.K., **2001**. A novel SnO_2/Al discrete gate ISFET pH sensor

with CMOS standard process. *Sensors and Actuators B: Chemical, 75*(1–2), pp.36–42.
14. Yuqing, M., Jianrong, C. and Keming, F., **2005**. New technology for the detection of pH. *Journal of Biochemical and Biophysical Methods, 63*(1), pp.1–9.
15. Knopfmacher, O., Tarasov, A., Fu, W., Wipf, M., Niesen, B., Calame, M. and Schonenberger, C., **2010**. Nernst limit in dual-gated Si-nanowire FET sensors. *Nano Letters, 10*(6), pp.2268–2274.
16. Park, J.K., Jang, H.J., Park, J.T. and Cho, W.J., **2014**. SOI dual-gate ISFET with variable oxide capacitance and channel thickness. *Solid-State Electronics, 97*, pp.2–7.
17. Yeo, J., Kim, G., Hong, S., Kim, M.S., Kim, D., Lee, J., Lee, H.B., Kwon, J., Suh, Y.D., Kang, H.W. and Sung, H.J., **2014**. Flexible supercapacitor fabrication by room temperature rapid laser processing of roll-to-roll printed metal nanoparticle ink for wearable electronics application. *Journal of Power Sources, 246*, pp.562–568.
18. Jang, H.J., Gu, J.G. and Cho, W.J., **2013**. Sensitivity enhancement of amorphous InGaZnO thin film transistor based extended gate field-effect transistors with dual-gate operation. *Sensors and Actuators B: Chemical, 181*, pp.880–884.
19. Lee, I.K., Lee, K.H., Lee, S. and Cho, W.J., **2014**. Microwave annealing effect for highly reliable biosensor: Dual-gate ion-sensitive field-effect transistor using amorphous InGaZnO thin-film transistor. *ACS Applied Materials & Interfaces, 6*(24), pp.22680–22686.
20. Lim, H.K. and Fossum, J.G., **1983**. Threshold voltage of thin-film silicon-on-insulator (SOI) MOSFET's. *IEEE Transactions on Electron Devices, 30*(10), pp.1244–1251.
21. Chi, L.L., Chou, J.C., Chung, W.Y., Sun, T.P. and Hsiung, S.K., **2000**. Study on extended gate field effect transistor with tin oxide sensing membrane. *Materials Chemistry and Physics, 63*(1), pp.19–23.
22. Batista, P.D. and Mulato, M., **2005**. ZnO extended-gate field-effect transistors as pH sensors. *Applied Physics Letters, 87*(14), p.143508.
23. Yin, L.T., Chou, J.C., Chung, W.Y., Sun, T.P. and Hsiung, S.K., **2000**. Separate structure extended gate H+-ion sensitive field effect transistor on a glass substrate. *Sensors and Actuators B: Chemical, 71*(1–2), pp.106–111.
24. Jang, H.J., Gu, J.G. and Cho, W.J., **2013**. Sensitivity enhancement of amorphous InGaZnO thin film transistor based extended gate field-effect transistors with dual-gate operation. *Sensors and Actuators B: Chemical, 181*, pp.880–884.
25. Valentini, L., Kenny, J.M., Alimenti, F. and Roselli, L., **2013**. Planar MOSFET devices on paper substrate using graphene oxide film as gate dielectric. *Microwave Conference (EuMC)*, October; European, IEEE. pp.5–8.
26. Kim, Y.H., Moon, D.G. and Han, J.I., **2004**. Organic TFT array on a paper substrate. *IEEE Electron Device Letters, 25*(10), pp.702–704.
27. Cho, W.J. and Lim, C.M., **2018**. Sensing properties of separative paper-based extended-gate ion-sensitive field-effect transistor for cost effective pH sensor applications. *Solid-State Electronics, 140*, pp.96–99.
28. Kim, J.Y., Park, S.H., Jeong, T., Bae, M.J., Song, S., Lee, J., Han, I.T., Jung, D. and Yu, S., **2010**. Paper as a substrate for inorganic powder electroluminescence devices. *IEEE Transactions on Electron Devices, 57*(6), pp.1470–1474.
29. Eder, F., Klauk, H., Halik, M., Zschieschang, U., Schmid, G. and Dehm, C., **2004**. Organic electronics on paper. *Applied Physics Letters, 84*(14), pp.2673–2675.
30. Chi, L.L., Chou, J.C., Chung, W.Y., Sun, T.P. and Hsiung, S.K., **2000**. Study on extended gate field effect transistor with tin oxide sensing membrane. *Materials Chemistry and Physics, 63*(1), pp.19–23.
31. Bousse, L. and Bergveld, P., **1984**. The role of buried OH sites in the response mechanism of inorganic-gate pH-sensitive ISFETs. *Sensors and Actuators, 6*(1), pp.65–78.
32. Brooke, B.S., Habashi, J.P., Judge, D.P., Patel, N., Loeys, B. and Dietz III, H.C., **2008**. Angiotensin II blockade and aortic-root dilation in Marfan's syndrome. *New England Journal of Medicine, 358*(26), pp.2787–2795.
33. He, X., Wang, L., Xiao, X., Deng, W., Zhang, L., Chan, M. and Zhang, S., **2014**. Implementation of fully self-aligned homojunction double-gate a-IGZO TFTs. *IEEE Electron Device Letters, 35*(9), pp.927–929.

Received: 27 July 2018. Accepted: 3 January 2019.